Biochemistry

 Volume 42, Number 2 January 21, 2003

Current Topics

Conformational Dynamics along an Enzymatic Reaction Pathway: Thymidylate Synthase, "the Movie"†

Robert M. Stroud* and Janet S. Finer-Moore

S-960 Department of Biochemistry and Biophysics, University of California in San Francisco, San Francisco, California 94143-0448

Received September 24, 2002; Revised Manuscript Received October 15, 2002

From crystal structures of thymidylate synthase (TS,[1] EC 1.1.45), we described the large conformational changes that take place upon binding of the substrate, dUMP, and a stable analogue of the cofactor, CH_2H_4folate, in atomic detail (*1*, *2*). The structural changes occur throughout the molecule and involve segmental accommodation, in which the entire protein adjusts to sequester the reactants from solution, rather than a domain motion. The question addressed here is how the progressive conformational changes that take place throughout the many-step reaction are coupled to function. It emerges that conformational dynamics is fundamental to the sequestration, and multistep reorientation necessary for the action of TS.

The chemical reaction, which lies at the end of the sole *de novo* pathway for synthesis of the DNA nucleotide dTMP, requires transfer first of a methylene group that lies between N5 and N10 of the cofactor to C5 of dUMP. Subsequent hydride transfer from the hydrogen at C6 of the cofactor to the methylene at C5 of dUMP reduces it to C5-methyl-dUMP, or dTMP. From more than 80 three-dimensional TS structures determined in our laboratory, it became clear that these two reaction steps, which form different covalent bonds, require a reorientation of the substrate and cofactor in the course of the reaction to permit both the methylene at N5 and the hydrogen at C6 of the cofactor to interact with C6 of the substrate, dUMP. Since the reaction involves several discrete chemical steps and requires reorientation of the substrate and enzyme at various stages, we sought to map the reaction pathway in structural terms, to understand the role of and control over structural transitions in TS.

The kinetic mechanism for ligand binding that was deduced from steady-state and pre-steady-state kinetics, secondary isotope effects, and chemical considerations provides a guide to the intermediates required to map the structural transitions of the reaction (Scheme 1) (*3*, *4*). This "guidepost" suggested that the enzyme binds dUMP first, before the physiologic form of the cofactor, in an ordered reaction. Certainly, the cofactor rapidly associates with the enzyme−nucleotide binary complex to form a loosely bound, noncovalent ternary complex. This is followed by a slow step coinciding with opening of the cofactor's five-membered imidazolidine ring which produces a reactive iminium ion. After ring opening occurs, covalent bonds are formed first between dUMP C6 and the active site sulfhydryl and, subsequently or simultaneously, between dUMP C5 and the cofactor methylene group.

We have used a series of crystal structures of *Escherichia coli* TS to obtain the stereochemical map of the reaction.[2] *E. coli* TS readily crystallizes as an apoenzyme and in binary and ternary complexes with the reactants or their analogues.

† Supported by National Institutes of Health Grant CA-41323.

* To whom correspondence should be addressed.

[1] Abbreviations: TS, thymidylate synthase; dUMP, 2′-deoxyuridine 5′-monophosphate; CH_2H_4folate or mTHF, 5,10-methylene-5,6,7,8-tetrahydrofolate; dTMP, 2′-deoxythymidine 5′-monophosphate; H_2folate or DHF, 7,8-dihydrofolate; H_4folate or THF, (6*S*)-5,6,7,8-tetrahydrofolate; FdUMP, 5-fluoro-dUMP; CB3717, 10-propargyl-5,8-dideazafolate; PABA, *p*-aminobenzoic acid.

[2] A movie derived from this series of structures showing TS conformational changes during the reaction is also available at http://msg.ucsf.edu/stroud/index.html.

10.1021/bi020598i CCC: $25.00
Published on Web 12/17/2002

Scheme 1

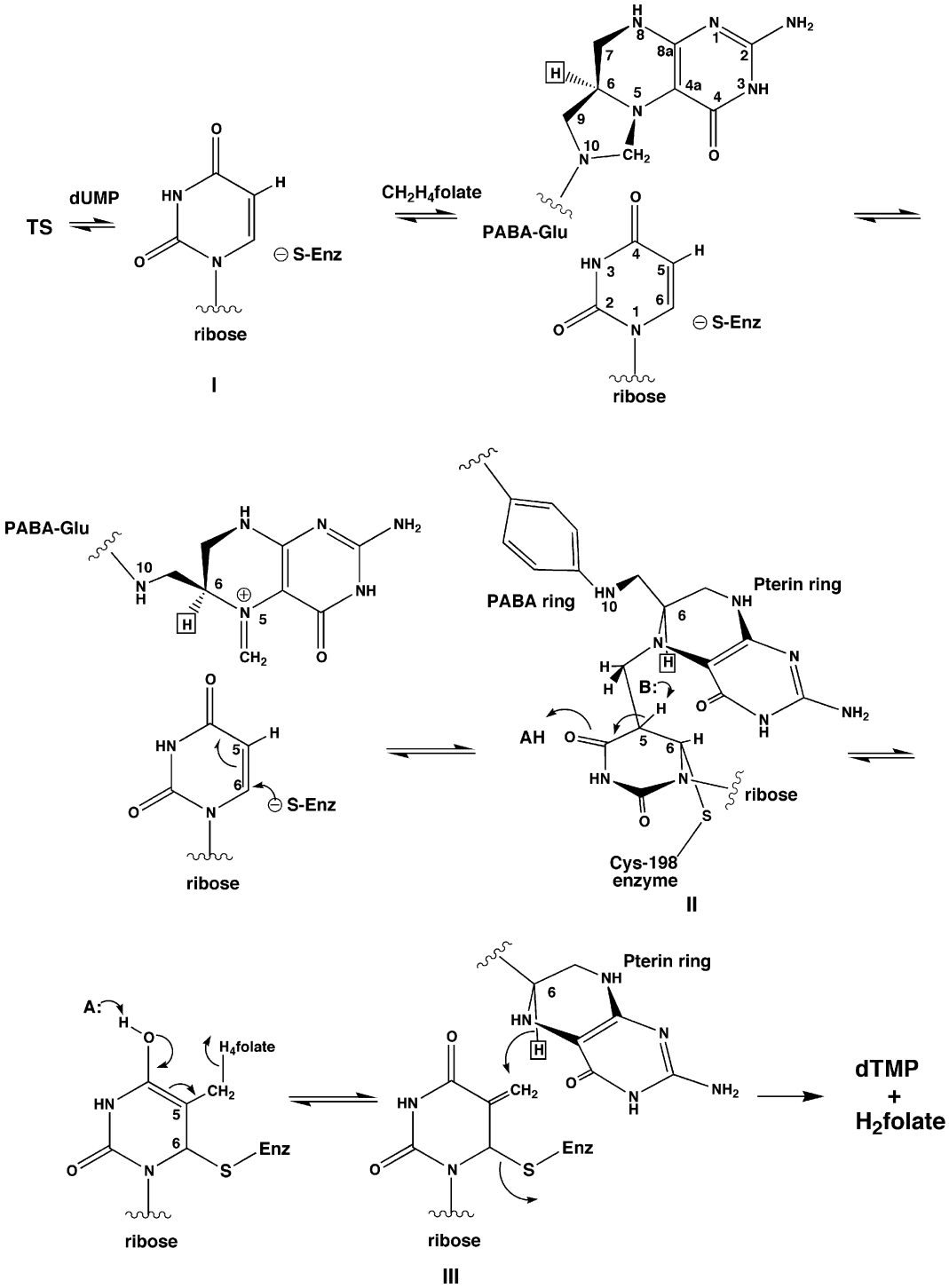

The crystal structures of the liganded forms of the *E. coli* enzyme have no disordered loops or domains, and *E. coli* TS crystals usually diffract to 2 Å resolution or better. A list of the structures is shown in Table 1.

Table 1: Analogues of Reaction Intermediates

crystal structure	reaction intermediate	resolution (Å)	R_{cryst}/R_{free} (%)
apo-TS (*7*)	(apo-TS)	2.2	19/24.3
TS−dUMP (*7*)	I	2.1	17.9/21.7
D169C−FdUMP−mTHF (*11*)	Ia	2.3	16.9/22.9
C146S−dUMP−mTHF	Ib	2.2	22
TS·dUMP·CB3717 (*1*, *7*)	II	2.0	17.2/22.1
TS·FdUMP·mTHF (*25*)	II	2.2	17.8
TS·dUMP·THF (*13*)	III	1.7	19.7/22.1
C146S·dTMP·DHF (*26*)	(product complex)	1.8	18.3

Snapshots of Sequential Ligand Binding in E. coli TS

In all species that have been studied, TS is an obligate dimer in which components of the active site derive from both subunits, at two equivalent interfaces on opposite sides of the molecule (Figure 1). The dimer interface is comprised of a back-to-back apposition of two six-stranded sheets with hydrophobic and hydrophilic contacts between them. It is unique in having a right-handed twist between the β-sheets (*5*, *6*) that is seemingly pinioned by the arrangement of

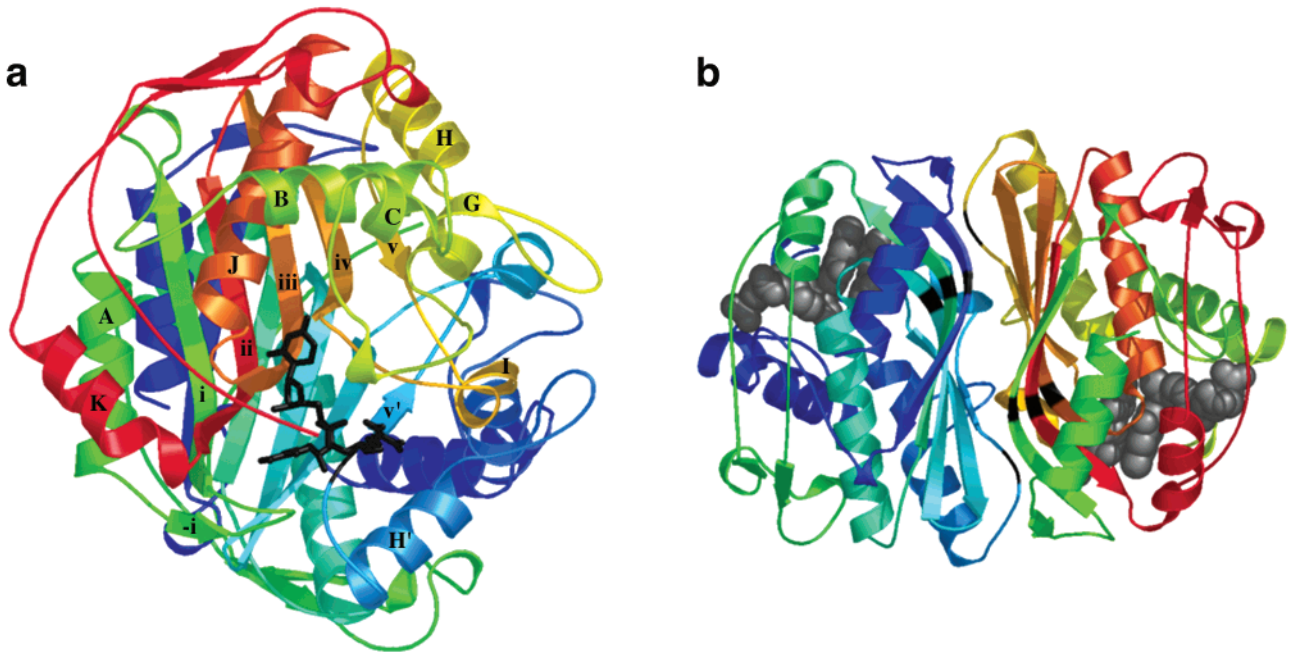

FIGURE 1: (a) Ribbon diagram of the *E. coli* TS dimer (PDB entry 2KCE), looking into the active site cavity of one of the protomers. Labels of helices and β-strands of this protomer correspond with the discussion in the text. Colors progress from blue at the N-terminus of the back protomer through the spectrum to red at the C-terminus of the front protomer. The substrate, dUMP, and the side chains contributed to this active site from the back protomer, Arg-178(126′) and Arg-179(127′), are shown as black sticks. The molecular 2-fold axis lies approximately in the plane of the paper, parallel to the horizontal dimension. (b) Ribbon diagram of the *E. coli* TS dimer rotated approximately 90° from panel a, with the 2-fold axis perpendicular to the plane of the paper. The color scheme is the same as in panel a except that Arg-178(126) and Arg-179(127) in both protomers and the β-kink residues in β-strands i−iii are black. Substrate, dUMP, and cofactor analogue, raltitrexed, are plotted as gray spheres. This figure was made with PyMOL from DeLano Scientific.

polar and nonpolar patches in the interface surfaces. The dimer interface enforces an unusual kink in the β-sheet at each active site that sharply bends the sheet to form one wall of the active site cavity (lower parts of strands i−iii in Figure 1).

dUMP binds to an essentially preformed binding site in the active site cavity of apo-TS. In the structure of the binary TS−dUMP complex, Arg-23(21)[3] and Arg-179′[4](127′) have switched to different side chain rotamers to contribute two hydrogen bonds from each side chain to the dUMP phosphate moiety (*7*). Side chains of residues Arg-178′(126′), Arg-218-(166), Ser-219(167), Asn-229(177), His-259(207), and Tyr-261(209), already positioned in the apoenzyme to hydrogen bond to dUMP, have not changed conformation.

According to the mechanism depicted in Scheme 1, the cofactor CH_2H_4folate binds to the dUMP complex with its imidazolidine ring closed. Opening of this ring is postulated to coincide with a transition to a closed enzyme conformation. To structurally isolate the initial weak adsorption ternary complex, we diffused the cofactor into crystals of the binary complex of *Lactobacillus casei* TS with dUMP (*8*). Lattice forces maintained the protein in an open conformation in these crystals. The structure of this complex showed the cofactor in its solution conformation, with its pterin ring approximately collinear with the PABA−Glu moiety, (*9*), bound to a conserved surface above the dUMP pyrimidine ring (Figure 2). If the protein would adopt the fully closed conformation seen in covalent ternary complexes of TS, Trp-82(80) would collide with the pterin ring of the cofactor bound at this site. CH_2H_4folate or its analogue CB3717 binds to this site in two *E. coli* TS mutants, E60(58)Q (*10*) and D221(169)N (*11*), in which the mutations prevent or dramatically slow the transition from the adsorption ternary complex to the closed covalent ternary complex.

The first chemically altered intermediate along the reaction pathway was mimicked by inactivation of TS by site-directed mutation, converting the active site nucleophile Cys-198-(146) to serine [C198(146)S]. Ser-198(146) can no longer participate in formation of a bond to dUMP by the usual Michael addition reaction. The structure of TS in this ternary complex has closed down around the substrate and cofactor relative to the structure of dUMP-bound or phosphate-inhibited TS. The four C-terminal residues have moved into the active site, a shift of ~5 Å, and two adjacent side chains, Trp-85(83) and Leu-195(143), have adopted different rotamer conformations to pack against the pterin ring. The backbone torsional angles of residues 23(21)−27(25) in the flexible loop containing phosphate-binding Arg-23(21) have changed with respect to those of the TS−dUMP complex, moving Thr-24(22) into the active site where Oγ1 donates a hydrogen bond to Oδ2 of Asp-22(20).

This structure also showed that the five-membered ring of the cofactor, which contains the methylene group for transfer, has opened, showing that either strain or chemical features of the site serve to predispose the cofactor to its subsequent reaction, even though there is no chemical bond formed to the substrate. The cofactor was trapped in the open ring form by reaction of the iminium ion with a molecule of water. Through adjustments to the dihedral angles of its pterin

[3] The numbering scheme of the *L. casei* enzyme is used. When a different species such as *E. coli* TS is discussed, its numbering is given in parentheses.

[4] Residues from the "second" monomer that enter into discussion of the "first" monomer are indicated with a prime, e.g., R178′.

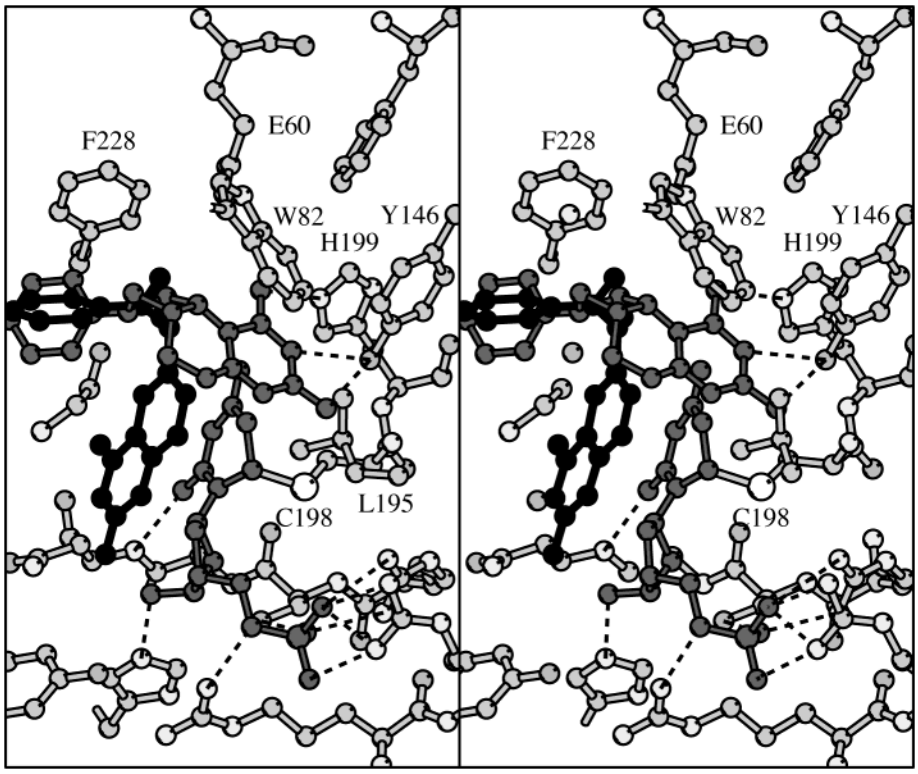

FIGURE 2: Stereoplot (*54*) of the active site of the *E. coli* TS D221N·FdUMP·CH_2H_4folate complex (*11*), with the protein shown in light gray and FdUMP and CH_2H_4folate in dark gray (the 5-fluorine of FdUMP is omitted from the plot). The CH_2H_4folate is in an extended conformation similar to that seen in solution (*9*), and it occupies an alternate binding site on the enzyme, which may be the initial cofactor "docking" site. For comparison of the docking and "productive" binding sites, CB3717 from the *E. coli* TS·dUMP·CB3717 complex is superimposed on the structure and plotted in black.

ring and rotations about its C6−C9 and C9−N10 bonds, the cofactor has transformed from an extended to a folded conformation in which its pterin ring is approximately perpendicular to its PABA moiety and parallel to and overlapping the pyrimidine ring of the bound dUMP. As expected, there is no covalent bond between dUMP and the enzyme. The extensive binding interface between dUMP and the cofactor in its opened ring, folded conformation explains why the cofactor binds much more tightly to the TS−dUMP binary complex than to the apoenzyme.

How the structure changes upon formation of the covalent addition complex between Cys-198(146) and C6 of dUMP is addressed with a third ternary complex formed with wild-type enzyme, dUMP, and a cofactor analogue that does not participate in methylene transfer, N10-propargyl-5,8-dideazafolate (CB3717) (*1*, *12*). The three-dimensional structure shows the quinazoline ring (analogous to the pterin ring of CH_2H_4folate) has moved far into the active site and made direct or water-mediated hydrogen bonds to Arg-23-(21), Asp-221(169), and the two C-terminal residues of the protein. Cys-198(146) Sγ has formed a covalent bond to C6 of dUMP by Michael addition. C5 of the quinazoline ring is positioned over C5 of the dUMP base; a pterin ring of the cofactor, so positioned, would be poised to form a covalent bond between its N5 methylene and C5 of dUMP. Overall, there is a net closure at this step with respect to the previous one.

The final step in forming the covalent ternary complex intermediate II involves covalent bond formation between C5 of dUMP and the N5 methylene of CH_2H_4folate. A close analogue of this structure is the complex formed by the active product of the anticancer drug fluorouracil (5-fluoro-dUMP). The electron withdrawing character of fluorine versus hydrogen at C5 does not allow for release of the fluorine. The structure remains trapped with covalent bonds formed between Cys-198(146) and C6 of dUMP, and between C5 of dUMP and the N5 methylene of the cofactor. The enzyme has not closed further in this final step, and the conformation of dUMP remains the same. The change from the flat benzene moiety of the quinazoline ring of CB3717 to the half-chair conformation of the unsaturated ring of the cofactor has positioned the methylene group at covalent bond distance from dUMP C5.

"Segmental Accommodation" in Response to Folate Binding

In summary, the TS reactants are first recruited to a large open highly conserved cavity which closes down progressively throughout the steps of the first half of the reaction, as delineated by the five complexes described above. During its initial binding to the apoenzyme, dUMP makes 13 hydrogen bonds, eight of them at the phosphate-binding site alone, and all of these hydrogen bonds are maintained throughout subsequent structural transitions. The enzyme hydrogen bonding groups Asn-229(177), His-259(207), and Tyr-261(209) track the position of dUMP as it moves toward the wall that contains Cys-198(146) during formation of the covalent ternary complex.

The conformational change is not a domain shift; rather, several segments of noncontiguous protein chain are moved in concert toward the active center against a stable protein

core, comprised largely of the dimer interface. The kink in strands i−iii of the β-sheet (Figure 1b) acts as one of several "hinge" points in the structure, about which other units in the protein rotate; the further from the hinge, the greater the displacement. Displacements range from ~0.3 Å near the hinge to 1.1 Å at the farthest residue from the active site, Gly-25(23), in the loop that contains phosphate-binding Arg-23(21).

A second hinge point lies at a bend in the central 21-residue J helix, which runs through the center of the protein (Figure 1a). The bend occurs at conserved Pro-227-(175), approximately two turns into the helix. The J helix lines one side of the active site cleft, and contacts the inhibitor at several points. The interaction with inhibitor results in a slight rotation of the helix and an increase in the helix bend, moving the amino end ~0.5 Å toward the active site. Moving along with the J helix are the three β-strands below and left of the β-kink. Residues attached to or packed with this portion of the β-sheet move along with it. For instance, the K helix, on the outside of the protein (Figure 1a), is displaced ~1.0 Å upon ligand binding.

On the right side of the molecule (as viewed in Figure 1a), the displacements are smaller. The β-bulge containing Cys-198(146), which initiates catalysis by nucleophilic attack on dUMP, is moved further into the active site. The angle between the B and C helices is altered slightly, and the loop connecting helix C to helix G has adjusted. This loop contains Trp-85(83), which hydrogen bonds to the C-terminus in the TS·dUMP·CB3717 complex but not in unliganded TS.

The most striking features of the conformational change are the shift of the four C-terminal residues into the active site and a conformational change to the loop containing Arg-23(21). These changes seal off one side of the active site cavity to bulk solvent and set up a network of hydrogen bonds to the pterin ring. Residues Trp-85(83) and Leu-195-(143) adopt different rotamers that serve to seal off the other side of the active site cavity (*13*). The new rotamer of Trp-85(83) helps immobilize the C-terminus by donating a hydrogen bond to the C-terminal carboxyl. Several segments of protein chain bearing hydrophobic residues shift by small amounts (approximately ≤1 Å) to bring the hydrophobic side chains into van der Waals contact with the cofactor (*1*).

EPR spectroscopy has shown that even in the absence of ligands, the C-terminus of TS is in equilibrium between the mobile, open conformation seen in crystal structures of the apoenzyme and the immobilized, closed conformation seen in ternary complex crystal structures, but that addition of cofactor or cofactor analogues dramatically shifts the equilibrium to the closed state (*14*). Complete closure of the active site through translations of multiple protein segments, as observed by ultraviolet absorbance spectroscopy (*15*−*17*) and hydrodynamics (*18*), occurs only when folate is bound. The forces that mediate closure may involve entropic factors associated with binding the hydrophobic components of the folate. The closure appears to be triggered by hydrophobic interactions with the PABA ring rather than hydrogen bonding to the C-terminus: TS is in the closed conformation in TS−CB3717 complexes in which the quinazoline ring of the antifolate does not interact with the C-terminus (*1*, *7*, *19*). Segmental shifts contributing to closure of the active site are required to bring residues Leu-224-(172), Ile-81(79), Phe-228(176), and Val-314(262) into contact with the PABA−Glu moiety.

Conformational change may also involve electrostatic factors. Two elliptical lobes of the enzyme that lie on opposite sides of the PABA ring of the substrate have opposite electrical charge, which suggests a mechanism for closure (*20*). These regions include segments that move significantly in response to ligand binding. In *E. coli* TS numbering, these residues include 48, 211−213, 215−222, (helix K), 255, and 257−261 (C-terminal tail) on one side and residues 57−59 (helix B), 61, and 66−90 (small domain) on the other. The difference in charge is conserved across species, suggesting that it plays a role in the mechanism of closure (*20*). The net charge on the N-terminal lobe (summarized across 28 species) is -3 ± 1, while it is 4 ± 1 on the C-terminal lobe. Thus, as the cofactor binds to TS, the dielectric constant within the cavity, close to 80 when filled with solvent, becomes closer to 2−4. The Coulombic electrostatic attractive force between two charged atoms on different lobes changes by ΔF ($\Delta F = q_1q_2/\epsilon_2 r_{12}^2 - q_1q_2/\epsilon_1 r_{12}^2 \sim q_1q_2/\epsilon_2 r_{12}^2$, where ϵ_1 is the dielectric constant in the solvent-filled active site cavity and ϵ_2 is the dielectric constant in the cofactor-bound active site cavity).

To roughly estimate the contribution these electrostatic factors could make in enzyme closure, Coulombic forces, $F = 1/\epsilon_2 \sum\sum (q_i q_j)/r_{ij}^2$, where i is summed over all atoms in the N-terminal lobe, j is summed over atoms in the C-terminal lobe, and a value of 4 was used for ϵ_2, were computed for apo-TSs from *E. coli*, *L. casei*, humans, *Bacillus subtilis*, and T4 phage. Values of F ranged from −2.5 kcal mol^{-1} Å^{-1} for *B. subtilis* TS to −7.0 kcal mol^{-1} Å^{-1} for human TS.

A Structural "Mechanism" for Docking and Orienting CH_2H_4folate in a Random Kinetic Mechanism

We mapped the first half of the reaction based on the presumed ordered, sequential binding mechanism shown in Scheme 1. However, our reaction snapshots are not inconsistent with a random kinetic mechanism, which is observed for *L. casei* TS and fetal pig liver TS under certain experimental conditions (*21*), since they reveal an initial docking site for cofactor that does not block the dUMP site (*8*, *11*) (Figure 2). Indeed, the antifolate, N10-propargyl-5,8-dideazafolate (CB3717), crystallized in a binary complex with *E. coli* TS, clearly occupies this docking site (*7*), indicating the feasibility of binding the cofactor before dUMP during catalysis. Random kinetics for TS occurs in phosphate buffer when a polyglutamylated CH_2H_4folate is used as the cofactor. Since polyglutamylation can increase the binding affinity of folates for TS by several 100-fold while phosphate anion competes with dUMP at the phosphate-binding site, these reaction conditions alter the relative binding affinities of the ligands.

Mapping the Second Half of the Reaction

The major conformational change the protein undergoes on forming a covalent ternary complex suggested the protein was flexible enough to accommodate large changes in ligand conformation and orientation throughout the reaction, and led to proposals for major reorientations of the cofactor at two steps after formation of intermediate II. First, the trans-

diaxial orientation of the catalytic sulfhydryl group and methylene bridge in intermediate II that was deduced from the crystal structures of its analogues was postulated to convert to a trans-diequatorial arrangement prior to breakdown of the covalent complex (*22*). The trans-diequatorial arrangement would permit a concerted elimination of the cofactor and H-C5 from dUMP, and would orient the transferred methylene group in a manner consistent with the stereospecificity of hydride transfer (*22*, *23*).

Second, it was proposed that after the cofactor was eliminated from intermediate II, its pterin ring would shift to a different binding site where Trp-82 would be optimally positioned to stabilize a putative radical cation intermediate in the hydride transfer step (*24*). Log(k_{cat}) values for a series of unnatural amino acid variants of Trp-82 in LcTS were strongly correlated with the theoretical ability of the substituted amino acids to bind Na^+, suggesting Trp-82 electrostatically stabilized a cationic intermediate in hydride transfer (*24*). However, occupation of this binding site requires conformational adjustments in a flexible loop of the protein.

While the postulated changes in ligand conformation and orientation are reasonable, they most probably do not occur. Crystal structures of analogues of reaction intermediates for late steps in the enzyme reaction have shown that after intermediate II forms, only minor changes to the protein conformation take place until products are released. The cofactor remains sequestered in a closed active site with little space for major reorientation. The crystal structure of *E. coli* TS in a ternary complex with dUMP and H_4folate, an analogue of intermediate III in Scheme 1, has a protein structure very similar to that of the *E. coli* TS·FdUMP·CH_2H_4folate complex (an analogue of intermediate II) but with the pterin ring shifted by approximately 1 Å such that the C6 hydrogen is positioned over the projected site of the C5 methylene group in the reaction intermediate (*13*). The precise repositioning of H-C6 over the site of transfer suggests that the hydride could be transferred in a single step, with Trp-82(80) stabilizing a positively charged transition state (*13*). Alternatively, hydride transfer may occur by two single-electron transfers as proposed previously (*23*, *24*), but with Trp-82(80) stabilizing the radical cation intermediate by long-range electrostatic effects.

Hyatt et al. (*25*) have modeled all intermediates in the TS reaction, adding their crystal structure of the TS·FdUMP·CH_2H_4folate complex as a model for intermediate II, and likewise concluded that major changes in protein conformation or ligand orientation are not required during breakdown of intermediate II or hydride transfer. In particular, they show that the stereospecificity of hydride transfer can be ascribed to a two-step (E1CB) elimination of first, dUMP H-C5 and then the cofactor from intermediate II, a mechanism which does not require conversion of the trans-diaxial orientation of the catalytic sulfhydryl and methylene bridge to a trans-diequatorial arrangement. Rehybridization of dUMP C5 during elimination of H-C5 reorients the methylene bridge such that the cofactor H-C6 will be transferred with the experimentally observed stereochemistry.

Product Release and Recycling

The protein conformation and ligand orientations in the crystal structure of the *E. coli* TS C198(146)S·dTMP·H_2-folate product complex are very similar to those observed in the TS·FdUMP·CH_2H_4folate complex (*26*). A steric clash between a conserved, ordered water molecule and the C5 methyl of dTMP may disfavor dTMP binding and facilitate product release. Since the *E. coli* TS product complex structure is fully closed, it provides no clues about the structural path that opens the active site to release the products and returns the protein to its apoenzyme structure. However, a crystal structure of *L casei* TS bound to products with the protein in an open conformation does suggest a possible pathway (*8*). The complex was made by diffusing the cofactor into crystals of an *L. casei* TS−dUMP complex, and allowing the enzyme reaction to take place within the crystal. The normally very weak crystal lattice forces are evidently sufficient to maintain the protein in the open conformation. Consequently, the PABA ring is not in close contact with protein residues, exhibits high thermal *B*-factors, and has moved partially out of the PABA binding site. The pterin ring of DHF is not stacked as closely against the pyrimidine ring of dTMP as in the closed *E. coli* TS product complex, and side chains of Arg-23(21) and Tyr-261(209), both nucleotide-binding residues, are rotated out of the active site. Thus, breaking of the hydrogen bonds made by the side chains of Arg-23(21) and Tyr-261(209) and reorientation of these side chains may be an early step in allowing DHF to exit the active site.

The Cofactor-Induced Conformational Change Is an Integral Part of Catalysis

Active Site Closure Aligns the Reactants. Most of the contacts between the cofactor and the protein are fully realized only in the closed enzyme conformation. These include hydrophobic interactions of the PABA and pterin rings with Ile-81, Trp-83, Trp-85, Leu-195, Leu-224, and Phe-228, and an elaborate hydrogen bond network between the protein C-terminus and the cofactor pterin ring mediated in part by three conserved waters. In crystal structures of TS ternary complexes in which dUMP and cofactor analogues are bound to partially open active sites, the hydrogen bond network may be present, but many of the hydrophobic contacts are not made, the cofactor analogue atoms have high *B*-factors, and their pterin-mimetic rings may be shifted 1−2 Å from productive alignment with dUMP (*13*). Typically, these partially open ternary complex structures have no covalent bond between the catalytic thiol and dUMP. This suggests that the first chemical step in catalysis is aided by precise alignment (within ∼1 Å) of the cofactor against dUMP, and this alignment, in turn, depends on the conformational change triggered by cofactor binding. A subsequent chemical step, hydride transfer to the methylene substituent at dUMP C5, also is sensitive to the alignment and reduction in mobility of the cofactor pterin ring (*13*).

An Essential Relay between the Substrate and a Catalytic Acid Is Established by Active Site Closure. Besides orienting the reactants, the conformational change also contributes to catalysis by positioning a general acid near the methyl transfer site. Closure of the active site cavity expels one or more waters near the site of methyl transfer as it brings together dUMP and the side chains of three highly conserved residues, Asn-229, Glu-60, and His-199, into a new hydrogen bond network (Figure 3). In the new hydrogen bonding scheme, the general acid Glu-60 is hydrogen bonded to dUMP via a conserved ordered water, a connection that is

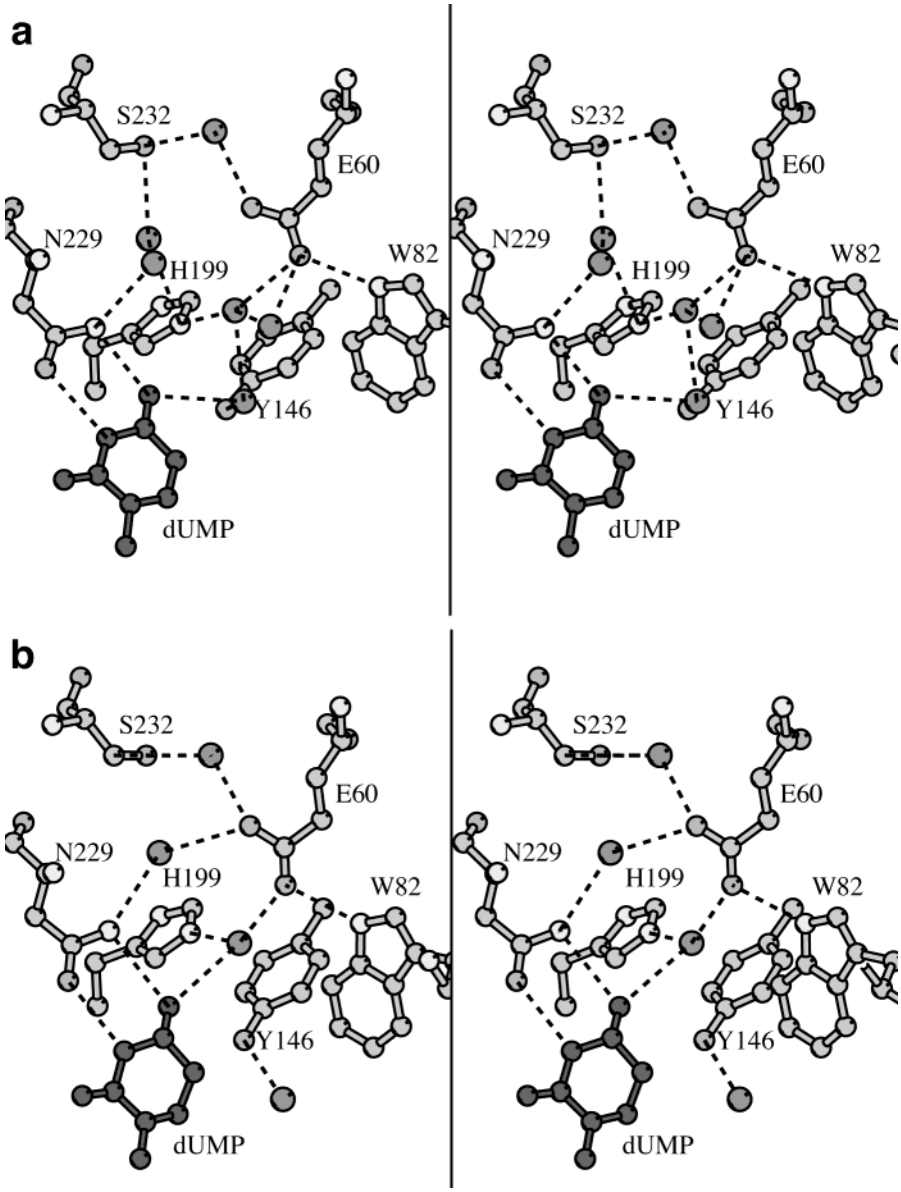

FIGURE 3: Stereoplots (*54*) of the water-mediated hydrogen bond networks connecting the general acid Glu-60 to O4 on the dUMP base in (a) the *E. coli* TS−dUMP binary complex (*7*) (open enzyme conformation) and (b) the *E. coli* TS·dUMP·CB3717 ternary complex (*1*) (closed enzyme conformation).

postulated to contribute to several steps that involve hydrogen transfers to and from the pyrimidine ring of dUMP (*10*, *27*). The hydrogen bonding potentials of all three side chains and dUMP are fully satisfied with hydrogen bonds of ideal geometry. This is a beautiful example of entropy−entropy compensation in which the cost of ordering the productive binding site is compensated by the replacement of bound water.

Conformational Change Is Postulated To Induce Strain that Contributes to Catalysis. A third way conformational change may contribute to catalysis is by forcing bound substrates into strained conformations that activate atoms on the substrate or cofactor. When the enzyme is in an open conformation, CH_2H_4folate with a closed imidazolidine ring can be positioned in the approximate binding site for the cofactor in the covalent ternary complex. However, closure of the active site forces the closed ring form of the cofactor into a strained conformation (*25*). The conformational strain is postulated to drive opening of the imidazolidine ring to produce the iminium ion intermediate that adds to C5 of dUMP to form the covalent ternary complex intermediate (*3*, *4*, *28*).

The conformational change also forces the ligands closer to the active site sulfhydryl in ternary complexes, promoting attack of the sulfhydryl on C6 of dUMP. The pyrimidine and ribose moieties of dUMP are ∼0.9 and ∼0.7 Å closer, respectively, to the catalytic cysteine in closed ternary complexes of *E. coli* TS than in binary *E. coli* TS−dUMP complexes (*7*).

After the covalent ternary complex is formed, Hyatt et al. postulate that geometric restrictions imposed by the protein structure weaken the covalent bond between C6 of dUMP and the catalytic cysteine (*25*). Weakening of the dUMP C6−Cys-198 Sγ bond in the ternary complex would make C5 of dUMP more electronegative, thereby facilitating abstraction of its hydrogen, a catalytic step required for elimination of the cofactor (*25*).

Structural Basis for Half-of-the-Sites Binding and Activity. Several kinetic and binding studies of different TS species indicate that both ligand binding affinity and enzyme activity are significantly higher for one of the protomers than for the second (*4*, *29*, *30*). In the case of *E. coli* TS (but not *L. casei* TS), mutant heterodimers with only one viable active site are as active as the wild-type enzyme, proving that *E. coli* TS has half-of-the-sites activity (*31*, *32*).

Crystal structures of ternary complexes of wild-type and mutant TSs show various degrees of asymmetry, ranging from different average *B*-factors in the two dimers (*1*) to different ligand occupancies (*33*). Evidence from these crystallographic studies suggests that the mechanism for asymmetric binding involves small structural changes at one protomer in response to ligand binding at the first (*33*). Since binding of cofactor or its analogues to TS induces shifts of several protein segments from disparate parts of the sequence, including segments at the dimer interface, it is not surprising that ternary complex formation in one protomer alters the structure and dynamics of the second. The asymmetric binding properties of folate analogue inhibitors vary: in the presence of dUMP, some antifolates do not bind asymmetrically to human TS, some bind more strongly to the first protomer, and some bind more strongly to the second (*29*). This is consistent with the notion that asymmetric binding results from relatively small conformational changes that, in optimizing binding interactions at one active site, change the environment of the second. Since the details of the conformational adjustments required to optimize protein−inhibitor contacts are different for each inhibitor, the inhibitors exhibit different types and degrees of cooperativity in binding.

The phenomena of asymmetric ligand binding affinity and half-of-the-sites activity are related by the intimate connections between substrate binding, conformational change, and alignment of ligands for methyl and hydride transfer reactions. In TS, binding energy pays the entropic cost of ligand alignment; thus, even if ligands were bound in the second site under physiological conditions, the weakened ligand binding affinity would result in a more open enzyme conformation, misalignment of ligands, and a reduction in k_{cat}.

Conformational Change in TSs of Other Species

The shifts of protein segments toward the active site cavity, which define the conformational change induced by binding of the cofactor or its analogues, are conserved among other TS species. The crystal structures of analogues of the covalent ternary complex intermediate II have been determined for *E. coli* (*34*, *35*), *Pneumocystis carinii* (*36*), *Cryptococcus neoformans*, humans (*37*, *38*), *B. subtilis* (*39*), and *L. major* (*40*) TSs, and structures have been determined for apo-TSs from *E. coli* (*41*), *L. casei* (*5*), T4 phage (*42*), *B. subtilis* (*43*), and humans (*44*, *47*, *48*). In all species, binding of folate analogues induces the conformational change. The apoenzymes and binary TS−dUMP complexes are always open, although the C-terminus is positioned in the active site cavity for some of these structures (*42*, *43*). However, rat and human TSs have both also been crystallized in an open conformation bound to dUMP and the antifolate raltitrexed (*45*−*47*), showing that the driving force for the conformational change is smaller in these species.

Flexible loops that change structure upon ligand binding are highly variable in structure among the apoenzymes, but adopt highly conserved conformations in covalent ternary complexes. Since the transition from the more mobile apoenzyme structure to the closed ternary complex conformation costs entropic energy, variations in apo-TS structures have implications for enzyme activity. Three versions of human TS that differ from the wild-type enzyme by deletions or insertions in the disordered N-terminal amino acid extension found in the human enzyme were crystallized in unliganded form and their crystal structures determined. One structure resembled the apo structures of other TS species (*47*). The other two structures were in an unusual conformation in which the active site loop that contains the catalytic cysteine is twisted almost 180° such that the cysteine points toward the dimer interface and is no longer in a position to interact with dUMP (*44*, *48*). Thus, the human apoenzyme may adopt a nonproductive conformation that must undergo a major conformational change to bind dUMP, and this may account for the low specific activity of human TS.

In *B. subtilis* TS-A, the "phosphate-binding loop" has an insert immediately after Arg-23(21) and Thr-24(22) that together with the two C-terminal residues form a short three-stranded β-sheet. The hydrogen bonds in the β-sheet maintain the loop in the same conformation as in the ternary complex. During closure of the enzyme, the loop and C-terminus shift essentially as a rigid body into the active site. Preordering of the C-terminus and phosphate-binding loop of *B. subtilis* apo-TS may contribute to the unusually high specific activity of this enzyme (*43*).

Implications of TS Dynamics for Drug Design

Mapping of the TS reaction has shown that TS has a structural core against which segments of secondary structure and flexible loops shift as the enzyme binds its substrates. Dozens of crystal structures of different TS species and their mutants, both in the apo form and bound to a variety of ligands, have now been determined and show that the same regions that respond to substrate binding also adapt their structures to engineered mutations, to sequence differences between species (including sequence inserts) (*41*), or to binding of novel inhibitors (*49*−*52*). These structures have been used to identify the most plastic regions of the protein (*36*, *52*). This information may be exploited in improving predictions of how small molecules may bind in the active site cavity of TS.

As a first pass at improving automated docking of small molecules to the active site of TS, a manifold of target structures was generated by assigning multiple rotamers to three active site residues (*36*). The side chains of the three residues had been found in a range of conformations in ligand-bound TS crystal structures. Docking against the target manifold dramatically improved predictions of the relative binding affinities of a set of ligands, and correctly identified known TS inhibitors that had been missed (i.e., were not among the top 500 compounds) when a single rigid target had been used (*36*).

The differences in the details of conformational flexibility among different species of TS may be useful in designing species-selective inhibitors. For example, the amino acid insertion at the β-kink in *P. carinii* TS allows the protein to adopt a novel conformation with a slightly larger active site

cavity (*53*). It is therefore absolutely clear that in the future, assessment of all the conformational states that can become accessible to a species of TS upon ligand binding must be an early step in *in silico* screening of potential novel inhibitors.

SUPPORTING INFORMATION AVAILABLE

A movie (used with the permission of R. M. Stroud) derived from this series of structures showing TS conformational changes during the reaction. This material is available free of charge via the Internet at http://pubs.acs.org.

REFERENCES

1. Montfort, W. R., Perry, K. M., Fauman, E. B., Finer-Moore, J. S., Maley, G. F., Hardy, L., Maley, F., and Stroud, R. M. (1990) *Biochemistry 29*, 6964−6977.
2. Finer-Moore, J. S., Montfort, W. R., and Stroud, R. M. (1990) *Biochemistry 29*, 6977−6986.
3. Santi, D. V., McHenry, C. S., Raines, R. T., and Ivanetich, K. M. (1987) *Biochemistry 26*, 8606−8613.
4. Spencer, H. T., Villafranca, J. E., and Appleman, J. R. (1997) *Biochemistry 36*, 4212−4222.
5. Hardy, L. W., Finer-Moore, J. S., Montfort, W. R., Jones, M. O., Santi, D. V., and Stroud, R. M. (1987) *Science 235*, 448−455.
6. Matthews, D. A., Appelt, K., and Oatley, S. J. (1989) *J. Mol. Biol. 205*, 449−454.
7. Stout, T. J., Sage, C. R., and Stroud, R. M. (1998) *Structure 6*, 839−848.
8. Birdsall, D. L., Finer-Moore, J., and Stroud, R. M. (1996) *J. Mol. Biol. 255*, 522−535.
9. Poe, M., Jackman, L. M., and Benkovic, S. J. (1979) *Biochemistry 18*, 5527−5530.
10. Sage, C. R., Rutenber, E. E., Stout, T. J., and Stroud, R. M. (1996) *Biochemistry 35*, 16270−16281.
11. Sage, C. R., Michelitsch, M. D., Stout, T. J., Biermann, D., Nissen, R., Finer-Moore, J., and Stroud, R. M. (1998) *Biochemistry 37*, 13893−13901.
12. Jones, T. R., Calvert, A. H., Jackman, A. L., Brown, S. J., Jones, M., and Harrap, K. R. (1981) *Eur. J. Cancer 17*, 11−19.
13. Fritz, T. A., Liu, L., Finer-Moore, J. S., and Stroud, R. M. (2002) *Biochemistry 41*, 7021−7029.
14. Carreras, C. W., Naber, N., Cooke, R., and Santi, D. V. (1994) *Biochemistry 33*, 2071−2077.
15. Danenberg, P. V., Langenbach, R. J., and Heidelberger, C. (1974) *Biochemistry 13*, 926−933.
16. Santi, D. V., McHenry, C. S., and Sommer, H. (1974) *Biochemistry 13*, 471−481.
17. Donato, H., Jr., Aull, J. L., Lyon, J. A., Reinsch, J. W., and Dunlap, R. B. (1976) *J. Biol. Chem. 251*, 1303−1310.
18. Lockshin, A., and Danenberg, P. V. (1980) *Biochemistry 19*, 4244−4251.
19. Kamb, A., Finer-Moore, J. S., and Stroud, R. M. (1992) *Biochemistry 31*, 12876−12884.
20. Fauman, E. B. (1995) Conformational Change and Catalysis in Thymidylate Synthase, Ph.D. Thesis, pp 118−122, University of California, San Francisco.
21. Ghose, C., Oleinick, R., Matthews, R. G., and Dunlap, R. B. (1990) in *Chemistry and Biology of Pteridines* (Curtius, H.-C., Ghisla, S., and Blau, N., Eds.) pp 860−865, Walter de Gruyter and Co., Berlin.
22. Matthews, D. A., Villafranca, J. E., Janson, C. A., Smith, W. W., Welsh, K., and Freer, S. (1990) *J. Mol. Biol. 214*, 937−948.
23. Slieker, L. J., and Benkovic, S. J. (1984) *J. Am. Chem. Soc. 106*, 1833−1838.
24. Barrett, J. E., Lucero, C. M., and Schultz, P. G. (1999) *J. Am. Chem. Soc. 121*, 7965−7966.
25. Hyatt, D. C., Maley, F., and Montfort, W. R. (1997) *Biochemistry 36*, 4585−4594.
26. Fauman, E. B., Rutenber, E. E., Maley, G. F., Maley, F., and Stroud, R. M. (1994) *Biochemistry 33*, 1502−1511.
27. Huang, W., and Santi, D. V. (1997) *Biochemistry 36*, 1869−1873.
28. Bruice, T. W., and Santi, D. V. (1982) *Biochemistry 21*, 6703−6709.
29. Dev, I. K., Dallas, W. S., Ferone, R., Hanlon, M., McKee, D. D., and Yates, B. B. (1994) *J. Biol. Chem. 269*, 1873−1882.
30. Variath, P., Liu, Y., Lee, T. T., Stroud, R. M., and Santi, D. V. (2000) *Biochemistry 39*, 2429−2435.
31. Maley, F., Pedersen-Lane, J., and Changchien, L. (1995) *Biochemistry 34*, 1469−1474.
32. Saxl, R. L., Changchien, L. M., Hardy, L. W., and Maley, F. (2001) *Biochemistry 40*, 5275−5282.
33. Anderson, A. C., O'Neil, R. H., DeLano, W. L., and Stroud, R. M. (1999) *Biochemistry 38*, 13829−13836.
34. Montfort, W. R., and Weichsel, A. (1997) *Pharmacol. Ther. 76*, 29−43.
35. Matthews, D. A., Appelt, K., Oatley, S. J., and Xuong, N. H. (1990) *J. Mol. Biol. 214*, 923−936.
36. Anderson, A. C., O'Neil, R. H., Surti, T. S., and Stroud, R. M. (2001) *Chem. Biol. 8*, 445−457.
37. Phan, J., Koli, S., Minor, W., Dunlap, R. B., Berger, S. H., and Lebioda, L. (2001) *Biochemistry 40*, 1897−1902.
38. Sayre, P. H., Finer-Moore, J. S., Fritz, T. A., Biermann, D., Gates, S. B., MacKellar, W. C., Patel, V. F., and Stroud, R. M. (2001) *J. Mol. Biol. 313*, 813−829.
39. Fox, K. M., Maley, F., Garibian, A., Changchien, L. M., and Van Roey, P. (1999) *Protein Sci. 8*, 538−544.
40. Knighton, D. R., Kan, C. C., Howland, E., Janson, C. A., Hostomska, Z., Welsh, K. M., and Matthews, D. A. (1994) *Nat. Struct. Biol. 1*, 186−194.
41. Perry, K. M., Fauman, E. B., Finer-Moore, J. S., Montfort, W. R., Maley, G. F., Maley, F., and Stroud, R. M. (1990) *Proteins 8*, 315−333.
42. Finer-Moore, J. S., Maley, G. F., Maley, F., Montfort, W. R., and Stroud, R. M. (1994) *Biochemistry 33*, 15459−15468.
43. Stout, T. J., Schellenberger, U., Santi, D. V., and Stroud, R. M. (1998) *Biochemistry 37*, 14736−14747.
44. Schiffer, C. A., Clifton, I. J., Davisson, V. J., Santi, D. V., and Stroud, R. M. (1995) *Biochemistry 34*, 16279−16287.
45. Jackman, A. L., Jodrell, D. I., Gibson, W., and Stephens, T. C. (1991) *Adv. Exp. Med. Biol. 309A*, 19−23.
46. Sotelo-Mundo, R. R., Ciesla, J., Dzik, J. M., Rode, W., Maley, F., Maley, G. F., Hardy, L. W., and Montfort, W. R. (1999) *Biochemistry 38*, 1087−1094.
47. Almog, R., Waddling, C. A., Maley, F., Maley, G. F., and Van Roey, P. (2001) *Protein Sci. 10*, 988−996.
48. Phan, J., Steadman, D. J., Koli, S., Ding, W. C., Minor, W., Dunlap, R. B., Berger, S. H., and Lebioda, L. (2001) *J. Biol. Chem. 276*, 14170−14177.
49. Weichsel, A., and Montfort, W. R. (1995) *Nat. Struct. Biol. 2*, 1095−1101.
50. Stout, T. J., Tondi, D., Rinaldi, M., Barlocco, D., Pecorari, P., Santi, D. V., Kuntz, I. D., Stroud, R. M., Shoichet, B. K., and Costi, M. P. (1999) *Biochemistry 38*, 1607−1617.
51. Stout, T. J., and Stroud, R. M. (1996) *Structure 4*, 67−77.
52. Fritz, T. A., Tondi, D., Finer-Moore, J. S., Costi, M. P., and Stroud, R. M. (2001) *Chem. Biol. 8*, 981−995.
53. Anderson, A. C., Perry, K. M., Freymann, D. M., and Stroud, R. M. (2000) *J. Mol. Biol. 297*, 645−657.
54. Kraulis, P. J. (1991) *J. Appl. Crystallogr. 24*, 946−950.

BI020598I